INORGANIC CHEMISTRY FRONTIERS

RESEARCH ARTICLE

View Article Online
View Journal

Cite this: DOI: 10.1039/d5qi01311a

$Y(C_6H_5SO_3)_3{\cdot}9H_2O$: strategic integration of ligand substitution and π-conjugated group linkage in sulfates for enhanced ultraviolet nonlinear optical properties

Xiaodong Zhang, [a,b] Bohui Xu, [a,b] Deshuai Xiao,[c] Xinyuan Zhang,[c] Pifu Gong *[a] and Zheshuai Lin *[a,b]

Received 16th June 2025,
Accepted 28th July 2025

DOI: 10.1039/d5qi01311a

rsc.li/frontiers-inorganic

Ultraviolet (UV) nonlinear optical (NLO) materials are critical for laser frequency conversion to extend wavelength ranges. Sulfates have emerged as a promising family of UV NLO materials, yet their NLO performance is constrained by the low optical anisotropy of the constituent $[SO_4]^{2-}$ groups. In this study, we investigate the $[C_6H_5SO_3]^-$ group, formed by substituting a ligand of the non-π-conjugated $[SO_4]^{2-}$ unit with a π-conjugated benzene ring, and demonstrate that this group has a strong second harmonic generation (SHG) response and large birefringence. Leveraging this optimized structural unit, we successfully synthesize the first UV NLO benzenesulfonate, $Y(C_6H_5SO_3)_3{\cdot}9H_2O$. This compound exhibits enhanced UV optical properties, including a short cutoff edge of 280 nm, a relatively large SHG efficiency (0.8 × KDP), and a large birefringence of 0.16 at 1064 nm. This work not only presents $Y(C_6H_5SO_3)_3{\cdot}9H_2O$ as a competitive UV NLO material, but also highlights the $[C_6H_5SO_3]^-$ group as a highly effective structural motif for the future development of advanced UV NLO materials.

Introduction

Nonlinear optical (NLO) crystals are indispensable materials for coherent laser frequency conversion, playing a pivotal role in the rapid development of laser technology and its diverse applications, including ultrafine spectroscopy, entangled photon pair generation, environmental monitoring, and explosive detection.[1–3] To date, commercial NLO materials such as LBO (LiB_3O_5),[4] β-BBO (β-BaB_2O_4),[5] KTP ($KTiOPO_4$),[6] KDP (KH_2PO_4)[7] and LN ($LiNbO_3$)[8] have demonstrated excellent performance, characterized by suitable transparency ranges, large second-harmonic generation (SHG) responses, and moderate birefringence. These properties stem from the well-arranged NLO-active units within their structures, as elucidated by, *e.g.*, anionic group theory.[9] However, as laser technology continues to evolve, the discovery of new NLO crystals with good performance has been imperative. Yet, surpassing the performance of commercial crystals using traditional structural units remains a great challenge. Thus, the development of new NLO active units is crucial for the exploration of next-generation NLO materials.[10–15]

Very recently, the non-π-conjugated $[SO_4]^{2-}$ unit has garnered significant attention owing to its ability to achieve wide bandgaps, strong SHG responses and rich structural diversity. For example, Zhao *et al.* reported $NH_4NaLi_2(SO_4)_2$,[16] which exhibits a bandgap of 5.5 eV and a SHG response of 1.1 × KDP. Similarly, Zou *et al.* demonstrated $CsSbF_2SO_4$[17] with a bandgap of 4.76 eV and a SHG response of 3 × KDP. Despite their promising properties, materials whose anionic groups are exclusively composed of non-π-conjugated $[SO_4]^{2-}$ groups typically exhibit low optical anisotropy. This is attributed to their nearly isotropic responses to external optical fields. This limitation typically results in small birefringence (~0.02), which would hinder the achievement of short phase matching wavelengths.

To address the challenge of low birefringence in sulfates, two primary strategies – typically employed separately – have been developed. The first strategy involves the incorporation of additional units with large structural anisotropy while maintaining the integrity of $[SO_4]^{2-}$ groups. For instance, planar π-conjugated groups, *e.g.*, the $[BO_3]^{3-}$ group, and stereochemically active lone pair (SCALP) cation-centred units, *e.g.*, the $[SbO_3Cl_2]$ group, have been successfully introduced into sulfates, achieving large birefringence values. Notable examples include $(NH_4)_2B_4SO_{10}$ (0.056 at 1064 nm)[18] reported by Pan

[a]Functional Crystals Lab, Technical Institute of Physics and Chemistry, Chinese Academy of Sciences, Beijing 100190, China
[b]University of Chinese Academy of Sciences, Beijing 100049, China
[c]Tianjin Key Laboratory of Functional Crystal Materials, Institute of Functional Crystals, Tianjin University of Technology, Tianjin 300384, China

et al. and $RbSbSO_4Cl_2$ (0.112 at 1064 nm)[19] reported by Zou *et al.* The second strategy focuses on enhancing polarizability anisotropy by modifying the ligands of the $[SO_4]^{2-}$ tetrahedron. Partial substitution of oxygen atoms in $[SO_4]^{2-}$ with other atoms or groups can disrupt the symmetry of the tetrahedron and deform its electron cloud structure, thereby improving polarizability anisotropy. This approach has led to the development of units such as $[SO_3F]^-$, $[SO_3CH_3]^-$, $[SO_3CF_3]^-$ and $[SO_3NH_2]^-$, which exhibit relatively large birefringence, enabling short phase-matching wavelengths in NLO sulfates. For example, Ye *et al.* reported $C(NH_2)_3SO_3F$[20] with a birefringence of 0.133; Lin *et al.* achieved a birefringence of 0.05 in $CsSO_3CF_3$ [21] and Luo *et al.* discovered $Sr(SO_3NH_2)_2$ [22] with a birefringence of 0.05.

In this work, we combine the two aforementioned strategies by substituting one oxygen atom in the $[SO_4]^{2-}$ tetrahedron with an additional group exhibiting large structural anisotropy, aiming to develop a new NLO active unit. Specifically, given its substantial hyperpolarizability, the planar π-conjugated benzene ring is chosen as the additional group. The $[C_6H_5SO_3]^-$ group, which fuses the π-conjugated benzene ring with the non-π-conjugated $[SO_4]^{2-}$ tetrahedron, is then constructed and subjected to theoretical investigation. This innovative group exhibits both large hyperpolarizability and significant polarizability anisotropy. Based on this optimized structural unit, we successfully synthesize the first UV NLO benzenesulfonate, $Y(C_6H_5SO_3)_3{\cdot}9H_2O$. This compound crystallizes in a non-centrosymmetric space group and exhibits a wide UV cutoff edge of 280 nm, a relatively large powder SHG response of 0.8 × KDP, a large birefringence of 0.16 at 1064 nm and a short phase matching wavelength of 300 nm, indicating its potential as a UV NLO material. Furthermore, first principles calculations are performed to elucidate its NLO mechanism, highlighting the $[C_6H_5SO_3]^-$ group as a promising NLO active unit for further exploration and material design.

Experimental section

Reagents

Benzenesulfonic acid (98%, Aladdin) and $YCl_3{\cdot}6H_2O$ (97%, Aladdin) were used directly in the synthesis process without further processing.

Synthesis

Benzenesulfonic acid (7.11 g, 4.5 mmol) was dissolved in 15 mL of deionized water. $YCl_3{\cdot}6H_2O$ (2.925 g, 1.5 mmol) was then added to the solution, and the mixture was stirred thoroughly until complete dissolution was achieved. The solution was permitted to evaporate gradually at a controlled temperature of 25 °C, which effectively facilitated the crystallization process. After a period of ten days, the formation of single crystals of $Y(C_6H_5SO_3)_3{\cdot}9H_2O$ was distinctly observed, as they precipitated and settled at the bottom of the beaker.

Single-crystal structure analysis

Single crystals of suitable dimensions (0.01 × 0.01 × 0.01 mm^3) were carefully selected for X-ray diffraction (XRD) analysis. Data collection was performed using a Bruker D8 Quest diffractometer equipped with a Mo Kα radiation source (λ = 0.71073 Å). Indexing and data integration were carried out using the APEX3 software suite, employing the difference vectors method. Absorption corrections were applied using the multi-scan method implemented in the SADABS program. The space group was determined using XPREP, which is integrated into the APEX3 package.[23]

The crystal structures were initially solved using SHELXT and subsequently refined with SHELXL-2014, employing full-matrix least-squares refinement on F^2. Anisotropic displacement parameters were included in this refinement process. The structural frameworks of $Y(C_6H_5SO_3)_3{\cdot}9H_2O$ were visualized and analyzed using the OLEX2 software package. The positions of individual atoms were refined by least-squares minimization using the SHELXL-2014 refinement package.[24] Finally, the PLATON program was used to verify the structural symmetry and authenticity.

Powder X-ray diffraction

The powder XRD (PXRD) measurements of $Y(C_6H_5SO_3)_3{\cdot}9H_2O$ were carried out on a Bruker D8 focus diffractometer (λ = 1.5418 Å and 2θ = 5–80°). The scanning step was set to 0.05°, and the fixed counting time was set to 0.5 s per step.

UV-vis-NIR diffuse reflectance spectra

The UV-vis diffuse reflection data were recorded at room temperature using powder samples and an Agilent Cary 7000 UV/vis/NIR spectrophotometer over 200–2000 nm. $BaSO_4$ was chosen as the back base.

Birefringence

Birefringence was measured using a Nikon Eclipse polarizing microscope E200MV POL under a visible light filter. The birefringence was calculated using the formula $\Delta n = \Delta R/T$, where ΔR, Δn, and T represent the optical path difference, the birefringence, and the thickness of the crystal, respectively. A transparent strip crystal was chosen to ensure accuracy. The thickness of the sample was measured using a Bruker Smart Apex II.

Thermal analysis

Thermogravimetric analysis (TGA) was performed on a HITACHI STA 200 instrument. The crystal sample was heated in the temperature range of 30–800 °C at a heating rate of 10 °C min^{-1}.

Powder SHG measurement

The powder SHG of $Y(C_6H_5SO_3)_3{\cdot}9H_2O$ was measured using the Kurtz–Perry approach[25] on a Q-switched Nd:YAG laser (1064 nm). Polycrystalline samples of $Y(C_6H_5SO_3)_3{\cdot}9H_2O$ were ground into different particle size ranges (10–60, 60–100,

100–150, and 200–250 μm). Accordingly, KH_2PO_4 (KDP) samples with the same particle size ranges were tested for reference.

Computational method

The electronic and optical properties of the $[C_6H_5SO_3]^-$ group and related $[SO_4]^{2-}$ based groups, including the LUMO–HOMO (lowest unoccupied molecular orbital–highest occupied molecular orbital) gaps, hyperpolarizability (β) and polarization anisotropy (δ) were investigated using Gaussian 16 software.[26,27] The calculations were performed using the B3LYP functional with the 6-31G basis set, a computational setting widely validated and employed in quantum chemical calculations.[28]

The CASTEP program based on density functional theory (DFT)[29] was employed to calculate the linear and nonlinear optical properties in $Y(C_6H_5SO_3)_3{\cdot}9H_2O$. The exchange–correlation (XC) functional is described by the generalized gradient approximation (GGA) with Perdew, Burke and Ernzerhof (PBE) functionals.[30] The ion/electron interactions are modelled using norm-conserving pseudopotentials for all the constituent elements. In this model, C $2s_22p_2$, H $1s_1$, O $2s_22p_4$, S $3s_23p_4$ and Y $4d_15s_2$ electrons are treated as the valence electrons. A kinetic energy cutoff of 750 eV and Monkhorst–Pack *k*-point meshes spanning less than 0.07 $Å^{-3}$ in the Brillouin zone were chosen to ensure sufficient accuracy for the present purposes.

The SHG coefficients were calculated using the method developed by our group. In addition, the band-resolved SHG coefficient and SHG-weighted density analyses were performed to intuitively visualize the electronic orbitals and structural motifs contributing to SHG in real space.[31] Our previous study revealed that the occupied-state contribution *via* virtual electronic transitions dominates the SHG effect in materials.[32]

Results and discussion

The $[C_6H_5SO_3]^-$ group can be viewed as a benzene ring replacing one O atom in the $[SO_4]^{2-}$ group. We theoretically investigated its LUMO–HOMO gap ($E_{LUMO-HOMO}$), hyperpolarizability (β) and polarization anisotropy (δ), and compared it with those in related $[SO_4]^{2-}$ based groups, including $[SO_4]^{2-}$, $[SO_3NH_2]^-$, $[SO_3F]^-$, and $[SO_3CH_3]^-$. Their structures and calculated results are shown in Fig. 1. As shown, the $[SO_4]^{2-}$, $[SO_3NH_2]^-$, $[SO_3F]^-$, and $[SO_3CH_3]^-$ groups exhibit a tetrahedral configuration, considering the small size of the H atom, while the $[SO_3CF_3]^-$ group adopts a distorted tetrahedral geometry. In comparison, the $[C_6H_5SO_3]^-$ group features a planar ring connected to a $[SO_3]$ triangular pyramid. These structural differences lead to significant variations in their optical properties. Notably, the NLO-related properties of the $[C_6H_5SO_3]^-$ group are studied for the first time, although its polarizability anisotropy has been previously highlighted.[33]

The results demonstrate that the $[C_6H_5SO_3]^-$ group exhibits superior β and δ, which are approximately two and ten times larger, respectively, than those of the related tetrahedral

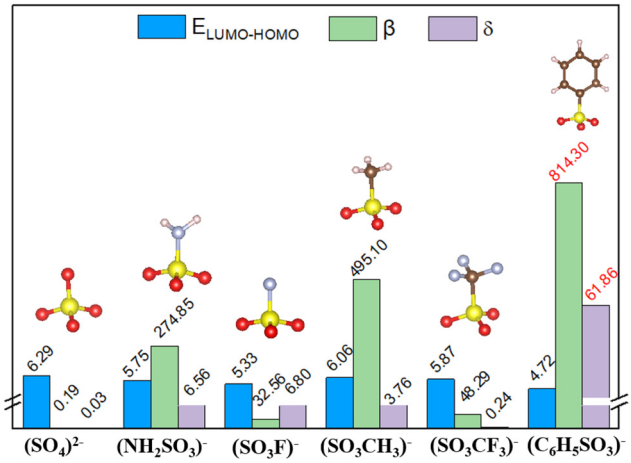

Fig. 1 Geometry and key NLO properties ($E_{LUMO-HOMO}$ (eV), β (a.u.) and δ (a.u.)) of $[SO_4]^{2-}$, $[SO_3NH_2]^-$, $[SO_3F]^-$, $[SO_3CH_3]^-$, $[SO_3CF_3]^-$ and $[C_6H_5SO_3]^-$.

groups. Meanwhile, a wide $E_{LUMO-HOMO}$ can be maintained even after the introduction of the π-conjugated benzene ring, which is conducive to applications in the UV range. These findings indicate that the incorporation of the $[C_6H_5]$ moiety significantly enhances the β and δ of the $[SO_4]^{2-}$ group, highlighting the $[C_6H_5SO_3]^-$ group as a promising UV NLO active group.

Based on the benzenesulfonic $[C_6H_5SO_3]^-$ unit, the first UV NLO benzenesulfonate, $Y(C_6H_5SO_3)_3{\cdot}9H_2O$, was successfully synthesized. Single crystals of $Y(C_6H_5SO_3)_3{\cdot}9H_2O$ were grown using a simple solution evaporation method and a single crystal with the dimensions of 10 × 10 × 2 mm^3 was obtained, as shown in Fig. 2a, which demonstrated a good crystal growth habit. Single-crystal XRD measurements were performed to solve and refine the crystal structure of $Y(C_6H_5SO_3)_3{\cdot}9H_2O$.

Detailed structural information including crystallographic data and refinement parameters, crystal data and structure

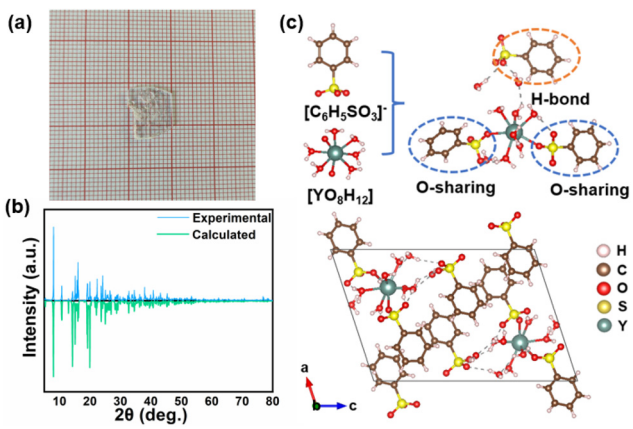

Fig. 2 (a) Single crystal photograph of a crystal of $Y(C_6H_5SO_3)_3{\cdot}9H_2O$. (b) Experimental and calculated XRD patterns of $Y(C_6H_5SO_3)_3{\cdot}9H_2O$. (c) Crystal structure of $Y(C_6H_5SO_3)_3{\cdot}9H_2O$.

refinement, atomic coordinates and equivalent isotropic displacement parameters, anisotropic displacement parameters, selected bond lengths, selected bond angles, and hydrogen atom coordinates with isotropic displacement parameters is provided in Table 1 and Tables S1–S6.

The PXRD pattern of the title compound is shown in Fig. 2b, which is in good agreement with the calculated results of the single crystal XRD data, indicating the high purity of the obtained samples. The crystal structure of $Y(C_6H_5SO_3)_3{\cdot}9H_2O$ is displayed in Fig. 2c. This compound crystallizes in the non-centrosymmetric monoclinic space group of $P2_1$ (no. 4). The asymmetric unit comprises 18, 33, 18, 3 and 1 crystallographically independent C, H, O, S and Y atoms, respectively. Six C and five H atoms constitute a benzene ring, which is further connected with $[SO_3]$ and forms a benzenesulfonic $[C_6H_5SO_3]^-$ unit. The Y atom is coordinated by eight O atoms, two of which originate from the $[C_6H_5SO_3]^-$ units, while the remaining six are provided by the H_2O molecule. As shown in Fig. 2c, the $[C_6H_5SO_3]^-$groups are connected to the Y atom in two ways: one is by sharing the oxygen atom on the $[C_6H_5SO_3]^-$ group, and the other is by hydrogen bonding mediated by water molecules nearby. The $[C_6H_5SO_3]^-$ groups are alternately arranged on the *a*–*c* plane, forming a porous structure. The $[YO_8H_{12}]$ groups occupy the space between coordination chains and hydrogen bonding in stabilizing the crystal structure.

Optical properties

The UV-vis diffuse spectrum of the title compound is displayed in Fig. 3a. Clearly, $Y(C_6H_5SO_3)_3{\cdot}9H_2O$ exhibits good transmittance extending into the UV region. Its UV cutoff edge is located at 280 nm, corresponding to a wide band gap of 4.35 eV,[34] indicating its potential for applications in the UV range. The UV cutoff edge of this compound is comparable to those of other UV NLO materials, such as $Li_2(H_2C_4N_2O_3){\cdot}2H_2O$ (260 nm),[35] $[C(NH_2)_3]_2SO_3S$ (254 nm),[36] and $[C(NH_2)_3]_3PO_4{\cdot}2H_2O$ (250 nm),[37] while it is smaller than those of $(NH_4)_2PO_3F$ (177 nm),[38] $Cs_3[(BOP)_2(B_3O_7)_3]$ (165 nm),[39] and $Rb_3B_{11}P_2O_{23}$ (168 nm).[40]

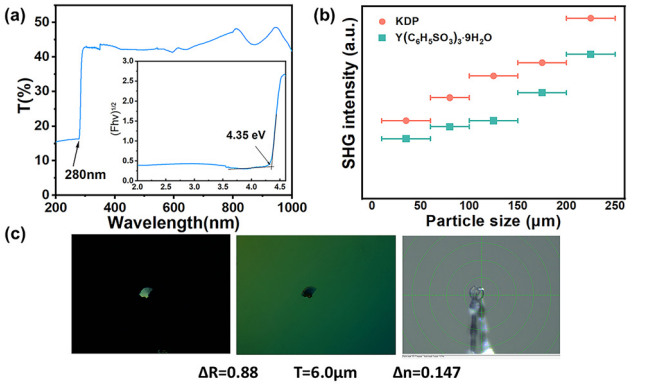

Fig. 3 (a) Transmittance of $Y(C_6H_5SO_3)_3{\cdot}9H_2O$. (b) SHG response of $Y(C_6H_5SO_3)_3{\cdot}9H_2O$. (c) Photos of a birefringence test of $Y(C_6H_5SO_3)_3{\cdot}9H_2O$.

The SHG response of $Y(C_6H_5SO_3)_3{\cdot}9H_2O$ was evaluated using the Kurtz–Perry method under 1064 nm laser irradiation, with KDP as the reference. As shown in Fig. 3b, the SHG signal of $Y(C_6H_5SO_3)_3{\cdot}9H_2O$ increases with particle size in the range from 10 to 250 μm, confirming its phase-matching capability. Finally, the SHG response reaches approximately 0.8 × KDP, a value comparable to those of $Ba_5P_6O_{20}$ (0.8 × KDP),[41] β-$(C_2H_5N_4)(NO_3)$ (0.8 × KDP),[42] and $K_7CaY_2(B_5O_{10})_3$ (1 × KDP),[43] and smaller than those of $Rb_3Hg_2(SO_4)_3Cl$ (1.5 × KDP)[44] and $NH_4B_4O_6F$ (3 × KDP).[45] It should be emphasized that, despite the large β of the $[C_6H_5SO_3]^-$ unit, the NLO-unfavorable arrangement of these units in $Y(C_6H_5SO_3)_3{\cdot}9H_2O$ may limit further enhancement of the SHG response.

The birefringence of $Y(C_6H_5SO_3)_3{\cdot}9H_2O$ was measured with a polarizing microscope (Fig. 3c). The optical path difference R was found to be 880 nm and the crystal thickness T was about 6.0 μm. Using the equation $\Delta n = \Delta R/T$, the birefringence was determined to be 0.147. This value exceeds those of commercial UV NLO materials, such as BBO[46] and LBO,[4] and is comparable to those of recently reported UV NLO materials, *e.g.*, $Zn(SCN)_2$ (0.164 at 546 nm),[47] $Na[BF_2(CN)_2]$ (0.152 at 546.1 nm),[48] and $Rb_2SbFP_2O_7$ (0.15 at 546 nm).[49] From a structural perspective, the large birefringence can be attributed to the planar arrangement of the π-conjugated benzene rings in $Y(C_6H_5SO_3)_3{\cdot}9H_2O$.

First-principles calculations were performed to evaluate the phase-matching behavior of $Y(C_6H_5SO_3)_3{\cdot}9H_2O$ (Fig. 4b). The calculated birefringence value at 1064 nm was 0.16, in good agreement with the experimental value. Based on the calculated refractive index dispersion curves, the shortest phase-matching wavelength was predicted to be 300 nm, indicating

Table 1 Crystallographic data and refinement parameters for $Y(C_6H_5SO_3)_3{\cdot}9H_2O$

	$Y(C_6H_5SO_3)_3{\cdot}9H_2O$
Formula	C18 H33 O18 S3 Y
fw	722.53
Crystal system	Monoclinic
Space group	$P2_1$
a/Å	11.8061(5)
b/Å	7.4977(2)
c/Å	17.4276(7)
α (°)	90
β (°)	108.183
γ (°)	90
V/Å^3	1472.34(10)
Z	2
D_c (g cm^{-3})	1.630
μ(Mo-Kα) (mm^{-1})	2.27
GOF on F^2	1.032
Flack factor	0.043(7)
R_1, R_2 ($I > 2\sigma(I)$)[a]	0.0406, 0.0748

[a] $R_1 = \sum||F_o| - |F_c||/\sum|F_o|$, $wR_2 = \{\sum w[(F_o)^2 - (F_c)^2]_2/\sum w[(F_o)^2]^2\}^{1/2}$.

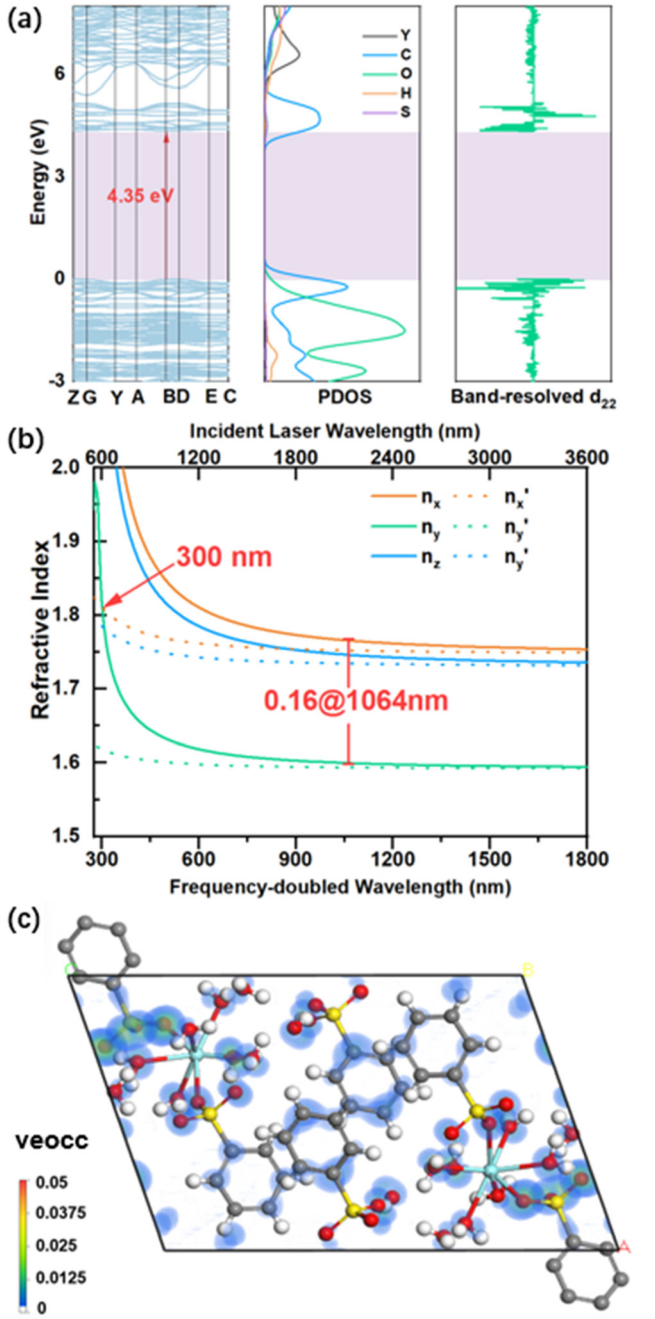

Fig. 4 (a) Calculated band structure, partial density of states, and band-resolved d_{22}. (b) Calculated refractive index and birefringence. (c) The VE-occupied SHG density.

its potential for NLO applications in the UV region. According to the Kleinman symmetry restriction, $Y(C_6H_5SO_3)_3{\cdot}9H_2O$ possesses four independent SHG coefficients, *i.e.*, d_{14}, d_{16}, d_{22} and d_{23}. The first-principles values were 0.07 pm V^{-1}, 0.29 pm V^{-1}, −0.50 pm V^{-1} and 0.04 pm V^{-1} for these SHG coefficients, respectively, with the maximum value of d_{22} = −0.50 pm V^{-1}, which agree well with the experimental result. To further elucidate the relationship between structure and NLO performance, the electronic band structure and partial density of states (PDOS) in $Y(C_6H_5SO_3)_3{\cdot}9H_2O$ were calculated, and the band-resolved analysis of the d_{22} coefficient was performed. As shown in Fig. 4a, $Y(C_6H_5SO_3)_3{\cdot}9H_2O$ is a direct bandgap compound. The orbitals located at both the conduction band minimum and the valence band maximum are occupied by O and C from the $[C_6H_5SO_3]^-$ group. Meanwhile, the band-resolved plot shows that the orbitals nearby the band gap play dominant roles in determining the SHG response, d_{22} in this case, indicating that the $[C_6H_5SO_3]^-$ group makes a dominant contribution to the NLO properties. To further clearly show the contributions of these orbitals, the SHG weighted densities are shown in Fig. 4c. Clearly, the orbitals are mainly from the $[C_6H_5SO_3]^-$ group. For further exploration, $[C_6H_5SO_3]^-$ groups may be used as good UV NLO active units and both larger SHG responses and birefringence are expected if they are arranged in an orderly manner.

Conclusions

In conclusion, the integration of a π-conjugated benzene ring into a non-π-conjugated $[SO_4]^{2-}$ tetrahedron led to the discovery of the $[C_6H_5SO_3]^-$ group as an exceptional UV NLO active unit, characterized by its large hyperpolarizability and significant polarizability anisotropy. Capitalizing on this discovery, we successfully synthesized the first UV NLO benzenesulfonate, $Y(C_6H_5SO_3)_3{\cdot}9H_2O$. This compound exhibits a wide bandgap, a relatively strong SHG response, a significant birefringence, and a short phase-matching wavelength, collectively highlighting its potential as a promising UV NLO material. Additionally, first-principles calculations were conducted to unravel the underlying NLO mechanism. This work not only introduces a new candidate for UV NLO materials but also establishes the $[C_6H_5SO_3]^-$ group as a high-performance UV NLO active unit for further exploration and material design.

Conflicts of interest

There are no conflicts of interest to report.

Data availability

The data supporting this article have been included as part of the SI.

TG/DTG curves of $Y(C_6H_5SO_3)_3{\cdot}9H_2O$, crystal data and structure refinement, atomic coordinates ($\times 10^4$) and equivalent isotropic displacement parameters ($Å^2 \times 10^3$), anisotropic displacement parameters ($Å^2 \times 10^3$), selected bond lengths, selected bond angles (deg), hydrogen atom coordinates ($Å \times 10^4$) and isotropic displacement parameters ($Å^2 \times 10^3$) of $Y(C_6H_5SO_3)_3{\cdot}9H_2O$. CCDC 2366861 contains the supplementary crystallographic data for this paper. See DOI: **https://doi.org/10.1039/d5qi01311a**.

CCDC 2366861 contains the supplementary crystallographic data for this paper.[50]

Acknowledgements

This work is supported by the National Natural Science Foundation of China (Grant No. 22275201 and 22133004). P. G. acknowledges support from the Youth Innovation Promotion Association CAS.

References

1 A. L. Cavalieri, N. Müller, T. Uphues, V. S. Yakovlev, A. Baltuška, B. Horvath, B. Schmidt, L. Blümel, R. Holzwarth, S. Hendel, M. Drescher, U. Kleineberg, P. M. Echenique, R. Kienberger, F. Krausz and U. Heinzmann, Attosecond spectroscopy in condensed matter, *Nature*, 2007, **449**, 1029–1032.

2 T. T. Tran, H. Yu, J. M. Rondinelli, K. R. Poeppelmeier and P. S. Halasyamani, Deep Ultraviolet Nonlinear Optical Materials, *Chem. Mater.*, 2016, **28**(15), 5238–5258.

3 X. Chen, H. Jo and K. M. Ok, Lead Mixed Oxyhalides Satisfying All Fundamental Requirements for High-Performance Mid-Infrared Nonlinear Optical Materials, *Angew. Chem., Int. Ed.*, 2020, **59**(19), 7514–7520.

4 C. Chen, Y. Wu, A. Jiang, B. Wu, G. You, R. Li and S. Lin, New nonlinear-optical crystal: LiB_3O_5, *J. Opt. Soc. Am. B*, 1989, **6**(4), 616–621.

5 C. Chen, Y. Wang, Y. Xia, B. Wu, D. Tang, K. Wu, Z. Wenrong, L. Yu and L. Mei, New development of nonlinear optical crystals for the ultraviolet region with molecular engineering approach, *J. Appl. Phys.*, 1995, **77**(6), 2268–2272.

6 Y. S. Liu, L. Drafall, D. Dentz and R. Belt, Nonlinear optical properties of $KTiOPO_4$ (KTP), [in] Proceedings of the Conference on Lasers and Electro-Optics, *OSA Technical Digest.*, 1981, WF4.

7 J. J. De Yoreo, Burnham A. K. and Whitman P. K. Developing KH_2PO_4 and KD_2PO_4 crystals for the world's most power laser, *Int. Mater. Rev.*, 2002, **47**(3), 113–152.

8 K. Guithi, H. E. Sekrafi, A. B. J. Kharrat, K. Khirouni and W. Boujelben, Synthesis, structural and optical characterization of $LiNbO_3$ material for optical applications, *J. Opt.*, 2023, **52**(3), 1494–1506.

9 C. Chen, Y. Wu and R. Li, The anionic group theory of the non-linear optical effect and its applications in the development of new high-quality NLO crystals in the borate series, *Int. Rev. Phys. Chem.*, 1989, **8**(1), 65–91.

10 L. Wu, C. Lin, H. Tian, Y. Zhou, H. Fan, S. Yang, N. Ye and M. Luo, *Angew. Chem., Int. Ed.*, 2024, **63**, e202315647.

11 L. Wu, C. Lin, H. Tian, T. Yan, X. B. Li, H. Fan, Y. Fan, S. Yang and M. Luo, *Angew. Chem., Int. Ed.*, 2025, **64**, e202500877.

12 D. Lin, M. Luo, C. Lin, F. Xu and N. Ye, *J. Am. Chem. Soc.*, 2019, **141**(8), 3390–3394.

13 Y. Deng, L. Huang, X. Dong, L. Wang, K. M. Ok, H. Zeng, Z. Lin and G. Zou, *Angew. Chem., Int. Ed.*, 2020, **59**, 21151.

14 Y. Tian, W. Zeng, X. Dong, L. Huang, Y. Zhou, H. Zeng, Z. Lin and G. Zou, *Angew. Chem., Int. Ed.*, 2024, **63**, e202409093.

15 X. Dong, L. Huang and G. Zou, *Acc. Chem. Res.*, 2025, **58**(1), 150–162.

16 Y. Li, F. Liang, S. Zhao, L. Li, Z. Wu, Q. Ding, S. Liu, Z. Lin, M. Hong and J. Luo, Two Non-π-Conjugated Deep-UV Nonlinear Optical Sulfates, *J. Am. Chem. Soc.*, 2019, **141**(9), 3833–3837.

17 X. Dong, L. Huang, C. Hu, H. Zeng, Z. Lin, X. Wang, K. M. Ok and G. Zou, $CsSbF_2SO_4$: An Excellent Ultraviolet Nonlinear Optical Sulfate with a $KTiOPO_4$ (KTP)-type Structure, *Angew. Chem., Int. Ed.*, 2019, **58**(20), 6528–6834.

18 Z. Li, W. Jin, F. Zhang, Z. Chen, Z. Yang and S. Pan, Achieving Short-Wavelength Phase-Matching Second Harmonic Generation in Boron-Rich Borosulfate with Planar $[BO_3]$ Units, *Angew. Chem., Int. Ed.*, 2022, **61**(4), e202112844.

19 F. He, Y. Deng, X. Zhao, L. Huang, D. Gao, J. Bi, X. Wang and G. Zou, $RbSbSO_4Cl_2$: an excellent sulfate nonlinear optical material generated due to the synergistic effect of three asymmetric chromophores, *J. Mater. Chem. C*, 2019, **7**(19), 5748–5754.

20 M. Luo, C. Lin, D. Lin and N. Ye, Rational Design of the Metal-Free $KBe_2BO_3F_2$·(KBBF) Family Member $C(NH_2)_3SO_3F$ with Ultraviolet Optical Nonlinearity, *Angew. Chem., Int. Ed.*, 2020, **59**(37), 15978–15981.

21 B. Xu, P. Gong, F. Liu, X. Zhang, H. Huo and Z. Lin, $(SO_3CF_3)^-$: A Non-π-Conjugated Motif for Nonlinear Optical Crystals Transparent into the Deep-Ultraviolet Region, *Adv. Opt. Mater.*, 2023, **12**(5), 2301725.

22 X. Hao, M. Luo, C. Lin, G. Peng, F. Xu and N. Ye, M $(NH_2SO_3)_2$ (M=Sr, Ba): Two Deep-Ultraviolet Transparent Sulfamates Exhibiting Strong Second Harmonic Generation Responses and Moderate Birefringence, *Angew. Chem., Int. Ed.*, 2021, **60**(14), 7621–7625.

23 G. M. Sheldrick, A short history of SHELX, *Acta Crystallogr., Sect. A:Found. Crystallogr.*, 2008, **64**, 112–122.

24 G. M. Sheldrick, Crystal structure refinement with SHELXL, *Acta Crystallogr., Sect. C:Struct. Chem.*, 2015, **71**, 3–8.

25 S. K. Kurtz and T. T. Perry, A Powder Technique for the Evaluation of Nonlinear Optical Materials, *J. Appl. Phys.*, 1968, **39**, 3798–3813.

26 R. Kumar, S. K. Yadav, R. Seth and A. Singh, Designing of gigantic first-order hyperpolarizability molecules via joining the promising organic fragments: a DFT study, *J. Mol. Model.*, 2023, **29**, 5.

27 I. Budagovsky, M. Smayev, A. Baranov, A. Kuznetsov, A. Zolot'ko and A. Bobrovsky, Optical anisotropy induced in amorphous azobenzene-containing polymers by light beams of various types, *Opt. Mater.*, 2024, **155**, 115823.

28 X. Wang, D. Toroz, S. Kim, S. L. Clegg, G.-S. Park and D. Di Tommaso, Density functional theory based molecular dynamics study of solution composition effects on the solvation shell of metal ions, *Phys. Chem. Chem. Phys.*, 2020, **22**(28), 16301–16313.

29 M. D. Segall, J. D. L. Philip, M. J. Probert, C. J. Pickard, P. J. Hasnip, S. J. Clark and M. C. Payne, First-principles simulation: ideas, illustrations and the CASTEP code, *J. Phys.:Condens. Matter*, 2002, **14**(11), 2717–2744.

30 J. P. Perdew, J. A. Chevary, S. H. Vosko, K. A. Jackson, M. R. Pederson, D. J. Singh and C. Fiolhais, Atoms, molecules, solids, and surfaces: Applications of the generalized gradient approximation for exchange and correlation, *Phys. Rev. B:Condens. Matter Mater. Phys.*, 1992, **46**(11), 6671–6687.

31 Z. Lin, X. Jiang, L. Kang, P. Gong, S. Luo and M.-H. Lee, First-principles materials applications and design of nonlinear optical crystals, *J. Phys. D:Appl. Phys.*, 2014, **47**(25), 253001.

32 R. He, Z. S. Lin, M.-H. Lee and C. T. Chen, Ab initio studies on the mechanism for linear and nonlinear optical effects in $YAl_3(BO_3)_4$, *Jpn. J. Appl. Phys.*, 2011, **109**(10), 103510.

33 Z. Bai and K. M. Ok, Designing Sulfate Crystals with Strong Optical Anisotropy through pi-Conjugated Tailoring, *Angew. Chem., Int. Ed.*, 2024, **63**(4), e202315311.

34 S. P. Tandon and J. P. Gupta, Measurement of Forbidden Energy Gap of Semiconductors by Diffuse Reflectance Technique, *Phys. Status Solidi B*, 1970, **38**(1), 363–367.

35 D. Lin, M. Luo, C. Lin, L. Cao and N. Ye, An Optimal Arrangement of $(H_2C_4N_2O_3)^{2-}$ Groups in the First Non-Centrosymmetric Alkali Barbiturate $Li_2(H_2C_4N_2O_3)\cdot 2H_2O$ Inducing a Giant Second Harmonic Generation Response and a Striking Birefringence, *Cryst. Growth Des.*, 2020, **20**(8), 4904–4908.

36 Y. Liu, X. Liu, Z. Xiong, B. Liu, J. Xu, L. Li, S. Zhao, Z. Lin, M. Hong and J. Luo, 2D van der Waals Layered $[C(NH_2)_3]_2SO_3S$ Exhibits Desirable UV Nonlinear-Optical Trade-Off, *Inorg. Chem.*, 2021, **60**(19), 14544–14549.

37 X. Wen, C. Lin, M. Luo, H. Fan, K. Chen and N. Ye, $[C(NH_2)_3]_3PO_4\cdot 2H_2O$: A new metal-free ultraviolet nonlinear optical phosphate with large birefringence and second-harmonic generation response, *Sci. China Mater.*, 2021, **64**(8), 2008–2016.

38 B. Zhang, G. Han, Y. Wang, X. Chen, Z. Yang and S. Pan, Expanding Frontiers of Ultraviolet Nonlinear Optical Materials with Fluorophosphates, *Chem. Mater.*, 2018, **30**(15), 2008–2016.

39 H. Liu, H. Wu, Z. Hu, J. Wang, Y. Wu and H. Yu, $Cs_3[(BOP)_2(B_3O_7)_3]$: A Deep-Ultraviolet Nonlinear Optical Crystal Designed by Optimizing Matching of Cation and Anion Groups, *J. Am. Chem. Soc.*, 2023, **145**(23), 12691–12700.

40 S. Wang, N. Ye, W. Li and D. Zhao, Alkaline Beryllium Borate $NaBeB_3O_6$ and $ABe_2B_3O_7$ (A = K, Rb) as UV Nonlinear Optical Crystals, *J. Am. Chem. Soc.*, 2010, **132**(25), 8779–8786.

41 S. Zhao, P. Gong, S. Luo, L. Bai, Z. Lin, Y. Tang, Y. Zhou, M. Hong and J. Luo, Tailored synthesis of a nonlinear optical phosphate with a short absorption edge, *Angew. Chem., Int. Ed.*, 2015, **54**(14), 4217–4221.

42 Q. Xia, X. Jiang, C. Jiang, H. Zhang, Y. Hu, L. Qi, C. Wu, G. Wei, Z. Lin, Z. Huang, M. G. Humphrey and C. Zhang, pH-Dependent Switching Between Nonlinear-Optical-Active Nitrate-Based Supramolecular Polymorphs, *Angew. Chem., Int. Ed.*, 2025, **64**, e202503136.

43 M. Mutailipu, Z. Xie, X. Su, M. Zhang, Y. Wang, Z. Yang, M. R. S. A. Janjua and S. Pan, Chemical Cosubstitution-Oriented Design of Rare-Earth Borates as Potential Ultraviolet Nonlinear Optical Materials, *J. Am. Chem. Soc.*, 2017, **139**(50), 18397–18405.

44 Y. Song, Y. Han, T. Yan and M. Luo, New Ultraviolet Nonlinear Optical Crystal $Rb_3Hg_2(SO_4)_3Cl$, *J. Inorg. Mater.*, 2023, **38**(7), 778–784.

45 G. Shi, Y. Wang, F. Zhang, B. Zhang, Z. Yang, X. Hou, S. Pan and K. R. Poeppelmeier, Finding the Next Deep-Ultraviolet Nonlinear Optical Material: $NH_4B_4O_6F$, *J. Am. Chem. Soc.*, 2017, **139**(31), 10645–10648.

46 R. Appel, C. D. Dyer and J. N. Lockwood, Design of a broadband UV-visible α-barium borate polarizer, *Appl. Opt.*, 2002, **41**(13), 2470–2480.

47 H. Zhang, X. Jiang, Y. Zhang, K. Duanmu, C. Wu, Z. Lin, J. Xu, J. Yang, Z. Huang, M. G. Humphrey and C. Zhang, Toward Strong UV–Vis–NIR Second-Harmonic Generation by Dimensionality Engineering of Zinc Thiocyanates, *J. Am. Chem. Soc.*, 2024, **146**(41), 28329–28338.

48 M. Y. Li, X. Liu, Y. C. Liu, R. X. Wang, J. Guo, L. M. Wu and L. Chen, Unprecedented Deep Ultraviolet (DUV) Birefringence in Fluorides Constructed from Linear π-Group Anisotropic Structure Building Units, *Angew. Chem., Int. Ed.*, 2025, **64**(8), e202423054.

49 X. Dong, H. Huang, L. Huang, Y. Zhou, B. Zhang, H. Zeng, Z. Lin and G. Zou, Unearthing Superior Inorganic UV Second-Order Nonlinear Optical Materials: A Mineral-Inspired Method Integrating First-Principles High-Throughput Screening and Crystal Engineering, *Angew. Chem., Int. Ed.*, 2024, **63**(11), e202318976.

50 X. Zhang, B. Xu, D. Xiao, X. Zhang, P. Gong and Z. Lin, CCDC 2366861: Experimental Crystal Structure Determination, 2025, DOI: **10.5517/ccdc.csd.cc2kfxc9**.